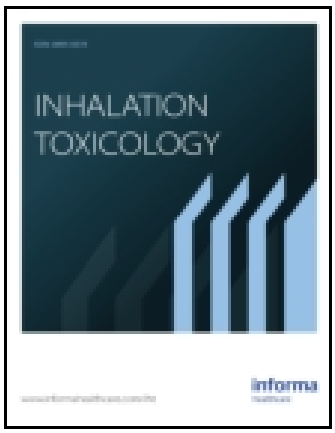

Inhalation Toxicology: International Forum for Respiratory Research
Publication details, including instructions for authors and subscription information:
http://www.tandfonline.com/loi/iiht20

Carbon nanotubes size classification, characterization and nasal airway deposition

Wei-Chung Su[a] & Yung Sung Cheng[a]
[a] Lovelace Respiratory Research Institute Albuquerque, NM 87108USA
Published online: 07 Oct 2014.

Inhalation Toxicology

http://informahealthcare.com/iht
ISSN: 0895-8378 (print), 1091-7691 (electronic)

Inhal Toxicol, 2014; 26(14): 843–852
 DOI: 10.3109/08958378.2014.960107

informa
healthcare

RESEARCH ARTICLE

Carbon nanotubes size classification, characterization and nasal airway deposition

Wei-Chung Su and Yung Sung Cheng

Lovelace Respiratory Research Institute, Albuquerque, NM 87108, USA

Abstract

Workers and researchers in the carbon nanotubes (CNT)-related industries and laboratories might be exposed to CNT aerosols while generating and handling CNT materials. From the viewpoint of occupational health, it is essential to study the deposition of CNT aerosol in the human respiratory tract to investigate the potential adverse health effects. In this study, a human nasal airway replica and two types of CNT materials were employed to conduct CNT nasal airway deposition studies. The two CNT materials were aerosolized by a nebulizer-based wet generation method, with size classified by three designated classification diameters (51, 101 and 215 nm), and then characterized individually in terms of their morphology and aerodynamic diameter. The nasal deposition experiments were carried out by delivering the size classified CNTs into the nasal airway replica in three different inspiratory flow rates. From the characterization study, it showed that the morphology of the size classified CNTs could be in a variety of complex shapes with their physical dimension much larger than their classification diameter. In addition, it was found that the aerodynamic diameters of the classified CNTs were slightly smaller than their classification diameter. The nasal deposition data acquired in this study showed that the deposition efficiency of CNTs in the nasal airway were generally less than 0.1, which implies that the majority of the CNTs inhaled into the nose could easily penetrate through the entire nasal airway and transit further down to the lower airways, possibly causing adverse health effects.

Keywords

Aerosol, carbon nanotubes, nasal airway

History

Received 8 July 2014
Revised 18 August 2014
Accepted 20 August 2014
Published online 7 October 2014

Introduction

Carbon nanotubes (CNT) are rolled graphene sheet with a cylindrical structure that can have a length to diameter aspect ratio of up to 10^8 (Wang et al., 2009). Based on the tube structure of the CNTs, several types of CNTs have been invented and manufactured. Examples such as single-walled nanotubes (SWCNTs), multi-walled nanotubes (MWCNTs) and stacked-cup carbon nanotubes (SCCNTs) are currently being produced and available in the market. CNTs have been widely applied in various commercial products because of their unique physical properties in terms of mechanical strength, thermal conductivity, electrical property and optical property (Endo et al., 2008). Based on published reports, the annual production capacity of CNT materials was 0.2 kiloton/year in 2005 and reached 4.6 kiloton/year in 2011 (De Volder et al., 2013). It was estimated that the total production value is expected to be 1.3 billion by 2015 (Parish, 2011).

Address for correspondence: Wei-Chung Su, Lovelace Respiratory Research Institute, 2425 Ridgecrest Dr. SE, Albuquerque, NM 87108, USA. Tel: +1 505 348 9571. Fax: +1 505 348 8567. E-mail: wsu@LRRI.org

CNT materials might become airborne in the CNT-associated workplaces and laboratories during handling, manufacturing, application and cleanup processes (Dahm et al., 2012; Chen et al., 2012). Therefore, those workers and researchers might be exposed to CNT aerosols, which could pose potential adverse health effects (Donaldson et al., 2006). Based on animal exposure studies in related literature (NIOSH, 2013), exposure to CNTs in mice can induce an early onset and persistence of pulmonary fibrosis (Porter et al., 2010), cause pulmonary inflammation (Muller et al., 2005) and reduce lung clearance function (Pauluhn, 2010). Animal studies also indicated that certain CNTs cause a burden to the macrophage in the alveoli or even migrate into the intrapleural space (Mercer et al., 2010). These findings raise a critical concern regarding the possible carcinogenicity of CNTs to induce lung cancer and pleural mesothelioma, the lung diseases which have been confirmed to be caused by notorious asbestos exposure (Peto et al., 1977). Therefore, studying the deposition of CNTs in the human airways is urgent and important from the point of view of occupational health and aerosol respiratory deposition to protect associated CNT workers. However, due to the fact that CNT aerosols are extremely small (in the nano-scale) and usually not a singular particle (but commonly aggregated together), there is a great uncertainty about the aerodynamic behavior as well as the

deposition efficiency of the CNT aerosols in the human airways. It is also very difficult to apply the traditional aerosol characterization and airway deposition scheme developed for micro-sized particles to the nano-sized CNTs for obtaining related physical characteristics and airway deposition data. As a result, to date no human airway deposition study has ever been carried out with CNTs. All published deposition data in the literature were limited to using isometric nanoparticles as test aerosols (Cheng et al., 1995; Kelly et al., 2004). Consequently, the deposition nature of CNTs in the human airway remains not well understood at present.

With this in mind, the purpose of this study was to carry out a series of *in vitro* CNT human airway deposition studies to acquire some original experimental data. The current study is the primary stage of the series of deposition studies designed and conducted in our laboratory. In this study, two CNT materials were aerosolized, size classified and characterized individually with unique methods and instruments especially suitable for nanoparticles to investigate the physical characteristics of the CNT aerosols. A realistic human nasal airway replica was employed for the deposition experiment since the nasal airway is an important entrance to the human respiratory tract. The CNT deposition efficiency obtained in the nasal airway can directly indicate the percentage of the inhaled aerosols that have then entered the lower airways. Therefore, studying the deposition of CNTs in the nasal airway is indispensable while investigating a whole picture of CNT respiratory deposition. The CNT nasal deposition data is also essential for developing and verifying a numerical model for estimating CNT airway deposition that can be used to assess the risk of the worker exposure to CNT in related occupational settings.

Experimental method

Nasal airway replica

A physical human nasal airway replica made of acrylic plates was used in this study. This nasal airway replica was made based on a set of *in vivo* head MRI scans of a nonsmoking Caucasian male (53 years of age, 73 kg in body mass and 173-cm tall). This nasal airway replica was constructed by 77 acrylic plates (1.5 mm thickness each) consisting of detailed nasal airway structures from the nostril, vestibule, nasal valve, turbinate and nasopharynx. The airway geometry and the flow field in this nasal airway replica have been well studied (Subramaniam et al., 1998; Zwartz & Guilmette, 2001), and this nasal airway replica has been used in many airway deposition studies with spherical particles or fiber aerosols in our laboratory (Cheng et al., 2001; Su & Cheng, 2005; Su et al., 2008). Figure 1 shows that the nasal airway replica used in this study. In this study, the inside surface of the nasal airway was applied with a layer of oil when conducting the deposition experiment to simulate the wet surface of a real human nasal airway.

CNT materials

Two CNT materials were employed in this study for the deposition experiment. One of the CNT materials was SCCNT (Shenzhen Nanotech Co., Shenzhen, China). This SCCNT material was engineered in high yield from a proprietary chemical vapor deposition process, and it has more than 95% purity with tube diameters around 10–20 nm and tube length about 5–15 μm before aerosolization. Figure 2(a) shows that the morphology of the SCCNT bulk material. This SCCNT material has been used in inhalation toxicology studies on mice (Mitchell et al., 2007). The other CNT used in this study was SWCNT material (SWeNT® SG76, Southwest NanoTechnologies, Norman, OK). Based on the manufacturer's specification, the SWCNT material has

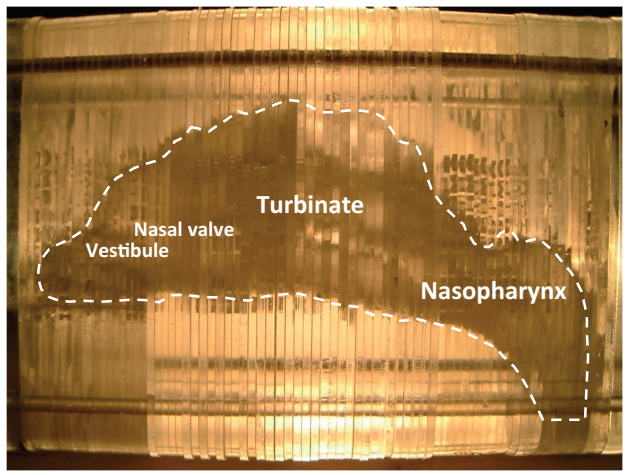

Figure 1. The human nasal airway replica.

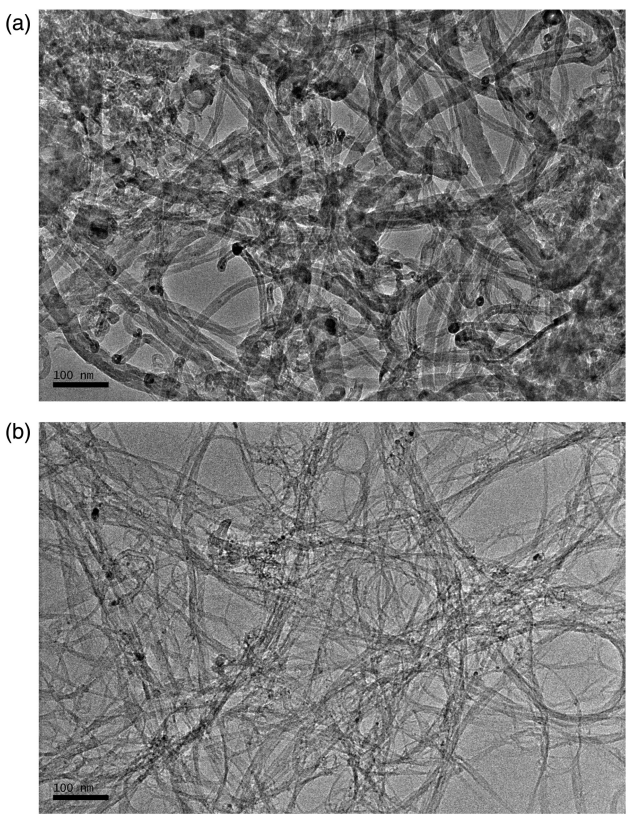

Figure 2. CNT materials used in this deposition study (a) stacked-cup carbon nanotubes (SCCNT) and (b) single-walled carbon nanotubes (SWCNT).

a tube diameter of 0.93 ± 0.27 nm with more than 90% carbon content by weight and high aspect ratio (>1000), which indicates that this SWCNT material has an elongated tube length. Figure 2(b) shows that the morphology of the SWCNTs used in this study.

CNT aerosol generation and characterization

Figure 3 shows that the experimental setup of the CNT aerosol generation, size classification and characterization scheme used in this study. In order to aerosolize the CNTs from the bulk material with a CNT aerosol concentration high enough for airway deposition study, a nebulizer-based wet method was adopted for generating CNT aerosols. To prepare CNT liquid suspension for the nebulizer, each CNT material was first put in optima® grad Isopropanol (Fisher Scientific, Pittsburgh, PA) and treated with an ultrasonicator for more than 24 h to break agglomerate and excessively long CNTs. The CNT suspension was then added into the nebulizer (Up-Mist, Hospitak Inc., Farmingdale, NY) for aerosol generation. In the generation system, three drying columns were installed to ensure the isopropanol mist would evaporate completely and only CNT aerosols would remain in the air flow for the deposition study. A Kr^{85} radioactive neutralizer was placed in the last drying column to have the CNT aerosols achieve charge equilibrium before being used further. It is believed that the CNT aerosols generated by this nebulizer-based wet generation method should be similar to those CNT aerosols generated by spray coating processes in some CNT application factories (Dahm et al., 2012).

In this study, the deposition experiment was designed to be conducted using size classified CNT aerosols. The preselected classification diameters for this study were 51, 101 and 215 nm. To classify CNT aerosols to the designated classification diameters, a differential mobility analyzer (DMA, Model 3071A, TSI Inc., Shoreview, MN) was used for this purpose. The principle of the DMA is to use the balance between the electrostatic force and the air drag force acting on the aerosols to size classify polydisperse aerosols into monodisperse aerosols according to the electrical mobility diameter (d_B) of the aerosols. Based on this mechanism, submicron and singly charged aerosols can provide the best condition for DMA operation. For size classifying CNT aerosols in this study, a portion (1 L/min) of the nebulizer-generated CNT aerosols was delivered into the DMA, and the DMA was set with parameters (sheath flow of 10 L/min and different voltages) to have CNT aerosols pass through the DMA and then be size classified based on their d_B. For measuring the size distribution of the size classified CNTs, the outlet of the DMA was connected to a sequential mobility particle sizer (SMPS) nanoparticle monitor (GRIMM Aerosol Technik GmbH & Co., Germany). Using the SMPS for size monitoring together with adjusting the DMA parameters, a desired concentration peak of the size classified CNTs can be ensured to locate at the designated classification sizes. In this study, samples of classified CNT aerosols were also collected on TEM grids based on each classification diameter using a point-to-plane electrostatic precipitator (In-Tox Products, Albuquerque, NM). The morphology of the classified CNTs was then inspected using a transmission electron microscope (TEM) examination (JEOL 2010, JEOL Ltd., Tokyo, Japan). Pictures of CNT aerosols in each classification diameter were taken while conducting the TEM morphology analysis.

In order to further understand the physical characteristics of the DMA classified CNT aerosols, the size classified CNTs were delivered to an aerosol particle mass analyzer (APM) equipment (Kanomax USA, Inc., Andover, NJ) for investigating associated effective density (ρ_{eff}) and aerodynamic diameter (d_{ae}). The d_{ae} is an aerosol physical property used for indicating aerosol inertia, which is also commonly used in plotting aerosol airway deposition results. The APM consists of two co-axis metal cylinders. The principle of the APM is to utilize the balance between the electrostatic force

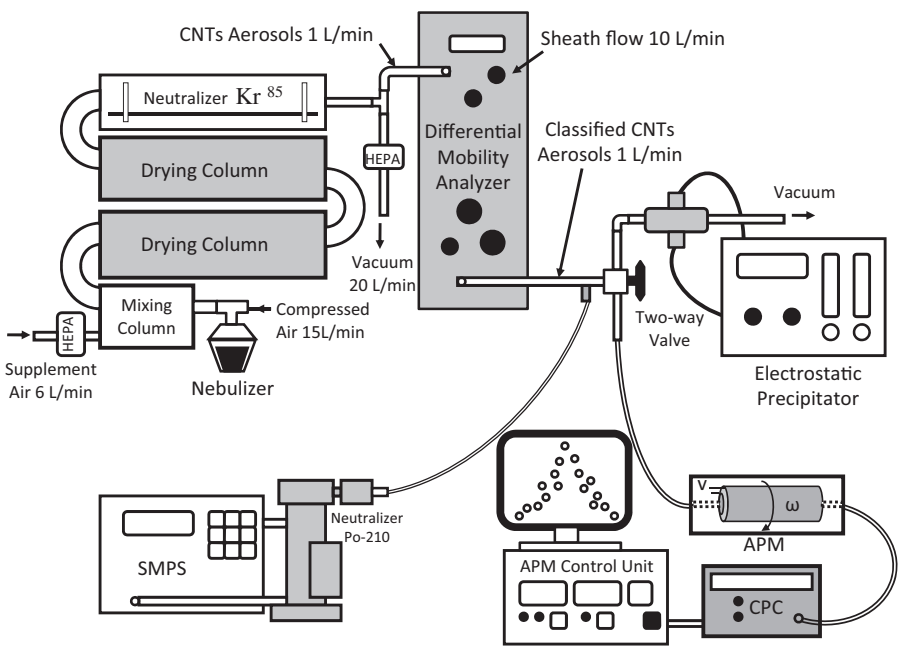

Figure 3. The experimental setup for the CNT aerosols generation, size classification and characterization.

(by changing voltage) and centrifugal force (by changing rpm) acting on the particles to acquire associated mass information for the test aerosol of interest. To use the APM to characterize the CNTs, the size classified CNTs were directly delivered into the APM after coming out of the DMA. In the APM, voltage corresponding to the peak aerosol concentration for a specific rpm in each test condition was measured and recorded. Monodispersed polystyrene latex (PSL, density = 1.02 g/cm^3) spheres with diameters close to the designated classification diameters of CNTs were employed as the reference particles in the APM study. In separate experiments, the PSL spheres were also aerosolized by the same nebulizer generation system, size classified by the DMA and then delivered into the APM for obtaining the reference voltage–concentration relationship. By comparing the voltage corresponding to the peak aerosol concentration between the classified CNTs and the reference PSL, the effective density of the classified CNTs, $\rho_{\text{eff, CNT}}$, can be calculated by the equation

$$\rho_{\text{eff,CNT}} = \rho_{\text{PSL}}\left(V_{\text{APM,CNT}/V_{\text{APM,PSL}}}\right), \quad (1)$$

where ρ_{PSL} is the density of the PSL. $V_{\text{APM, CNT}}$ and $V_{\text{APM, PSL}}$ are the voltage corresponding to the peak aerosol concentrations for classified CNTs and PSL, respectively. Once the effective density of the classified CNTs was available, the d_{ae} of the classified CNTs can then be calculated by solving the equation

$$\rho_{\text{o}} d_{\text{ae}}^2 C(d_{\text{ae}}) = \rho_{\text{eff,CNT}} d_{\text{B}}^2 C(d_{\text{B}}), \quad (2)$$

where ρ_{o} is the unit density, C (d_{ae}) is the aerosol slip correction factor for the classified CNTs with aerodynamic diameter d_{ae} and C (d_{B}) is the aerosol slip correction factor for a particle with electrical mobility diameter of d_{B} (the designated classification diameter). It is worth noting that the experimental setup, procedure and equations described above and used in the APM study to characterize the size classified CNTs have already been well established and applied in many researches to study the ρ_{eff} and d_{ae} for nanoparticles (McMurry et al., 2002; Park et al., 2003; Ku et al., 2006).

Nasal airway deposition experiments

The CNT nasal deposition experiment was conducted by delivering DMA size classified CNTs into the nasal airway replica and measuring the CNT concentrations both at the inlet and outlet of the nasal airway replica. Figure 4 demonstrates the experimental setup of the nasal airway deposition study. Inspiratory flow rates of 15, 30 and 43.5 L/min were used in this deposition study. These three flow rates represent the breathing flow rate of a worker having a light, intermediate and heavy workload, respectively (NCRP, 1997). For measuring the CNT concentration at the inlet and outlet of the nasal airway replica, a SMPS was connected to the inlet and outlet of the nasal airway replica and a two-way valve was used to facilitate switching between the two measurement taking locations. As mentioned previously, the size classified CNT aerosols would present a peak concentration right at the channel bar corresponding to the designated classification diameter. Therefore, when conducting the CNT deposition experiment for a certain classification diameter, only that single channel bar showing the peak concentration was used in the study to track the varying of the CNT concentration over time. Figure 5(a) shows an example of the SMPS data from a real deposition study. As can be seen, the SMPS measure the concentration of the size classified CNT for every second over time, and the abrupt concentration change in Figure 5(a) indicates the measurement taking was switched from the inlet to the outlet of the nasal airway. The SMPS instrument raw data can be exported to MS Excel, and then the average concentration at the inlet and outlet of the nasal airway replica can be estimated. Figure 5(b) shows the estimated CNT average concentration at the inlet and outlet of the nasal airway. With

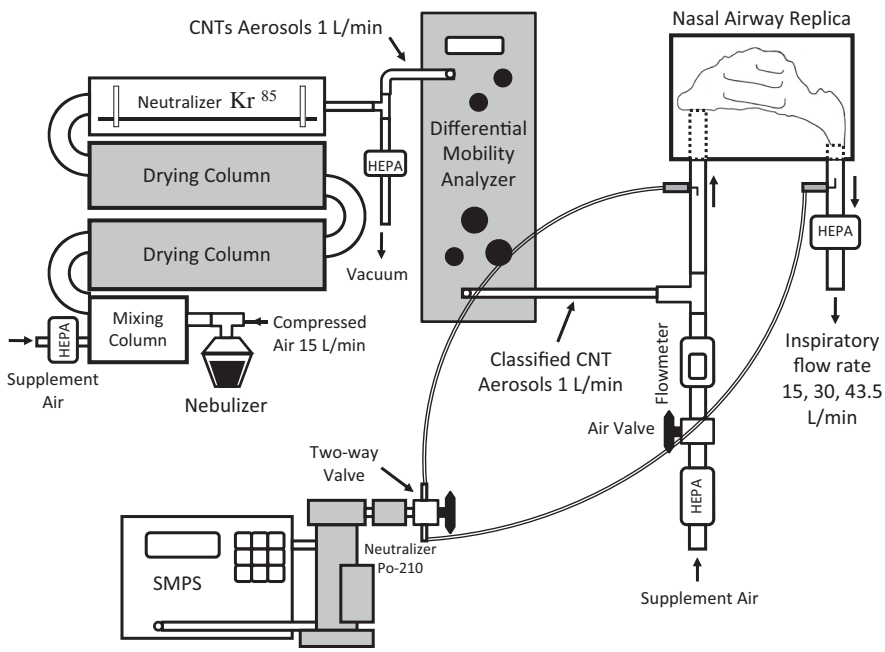

Figure 4. The experimental setup of the nasal airway deposition study using size classified CNTs.

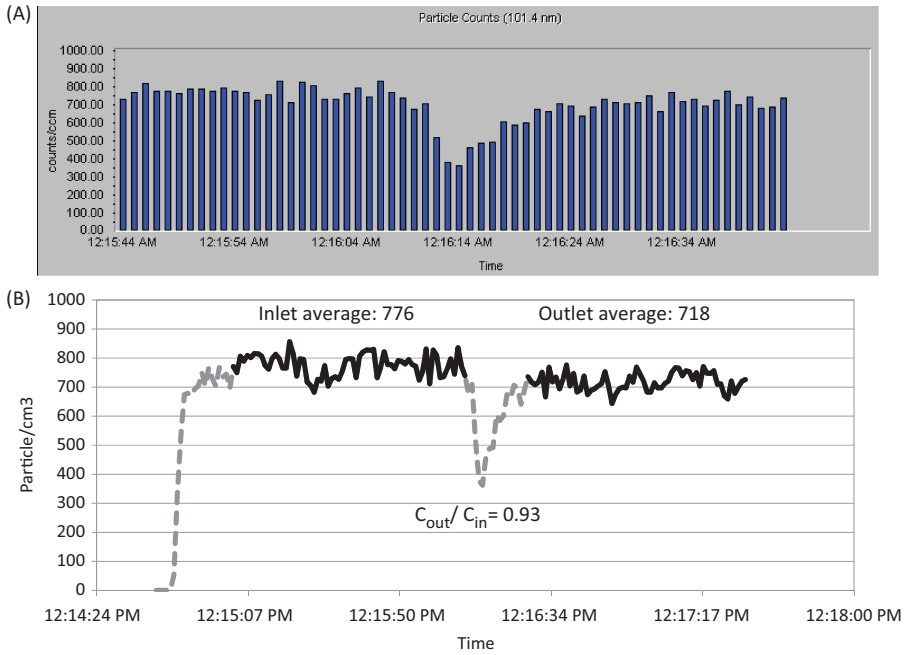

Figure 5. The concentration measurement of classified CNTs at the inlet and outlet of the nasal airway replica (a) instrument raw data and (b) average concentration.

the average CNT concentrations available both at the inlet and outlet of the nasal airway, the nasal deposition efficiency of a size classified CNT can be determined by the equation

$$\mathrm{DE} = 1 - F(C_{\mathrm{out}}/C_{\mathrm{in}}), \quad (3)$$

where DE is the nasal deposition efficiency of the size classified CNT, C_{in} and C_{out} are the average number concentration (particle/cm^3) of the size classified CNTs measured at the inlet and outlet of the nasal airway replica, respectively. F is the particle delivery efficiency correction factor (to be defined afterward) for a certain experimental condition. In this study, each experimental condition (arranged with two CNT materials, three classification diameters and three flow rates) was repeated at least five times for obtaining statistically meaningful deposition results.

Since the CNT aerosols used in this deposition study were in the nano-scale, systemic error due to diffusion wall loss while CNT aerosols are transiting in the tubing installed in the experimental setup might be a concern. In order to take into account systemic error and more accurately estimate the nasal deposition efficiency, studies were carried out to investigate the particle delivery efficiency correction factor for the experimental setup used in this deposition study. The particle delivery efficiency correction factor investigation was conducted by using the same experimental setup described above for nasal deposition study, but without the physical nasal airway replica installed. The CNT concentration ratio $C_{\mathrm{out}}/C_{\mathrm{in}}$ was measured by the SMPS, again both at the inlet and outlet locations of the experimental setup (the inlet and outlet were connected directly to each other). The particle delivery efficiency correction factor, F, is defined as the inversion of the concentration ratio measured by the SMPS ($F = C_{\mathrm{in}}/C_{\mathrm{out}}$). The particle delivery efficiency correction factor investigation was conducted for each experimental condition designed in the nasal deposition study. The particle delivery efficiency correction factors acquired were then applied to Equation (3), functioning to adjust the CNT concentration ratio $C_{\mathrm{out}}/C_{\mathrm{in}}$ measured in the real nasal deposition experiment when the nasal airway was installed. In this way, it is believed that the nasal deposition data acquired in this study is more precise and close to the true nasal deposition efficiency with the particle delivery efficiency correction factor taken into account.

Results

Figure 6 shows the size distribution of the SCCNT and SWCNT aerosols before and after the size classification measured by the SMPS. As can be seen, the size classified CNTs showed an ideal concentration peak right at the SMPS channel bar representing the designed classification diameter (51, 101 and 215 nm). Figures 7 and 8 demonstrate some morphology examples of the size classified SCCNT and SWCNT aerosols collected by the electrostatic precipitator. It can be seen that the morphology of the SCCNT and SWCNT aerosols were noticeably distinct. Most of the size classified SCCNT aerosols still show to a certain extent a fiber-like morphology. On the other hand, all of the size classified SWCNT aerosols were found to be similar to a twisted rubber band. Figure 9 displays some results of the voltage–concentration measurement acquired from the APM study for size classified SCCNT and SWCNT aerosols, as well as for the PSL reference particle. Table 1 presents the effective densities and aerodynamic diameters of the size classified SCCNTs and SWCNTs calculated by Equations (1) and (2). It can be seen that the estimated d_{ae} of the size classified CNT aerosols were generally less than their d_{B} (classification diameter). Table 1 also shows that the larger the CNT aerosol, the less d_{ae} than d_{B}. Table 2 shows the deposition efficiencies of CNT in the nasal airway obtained for different CNT materials, classification sizes and

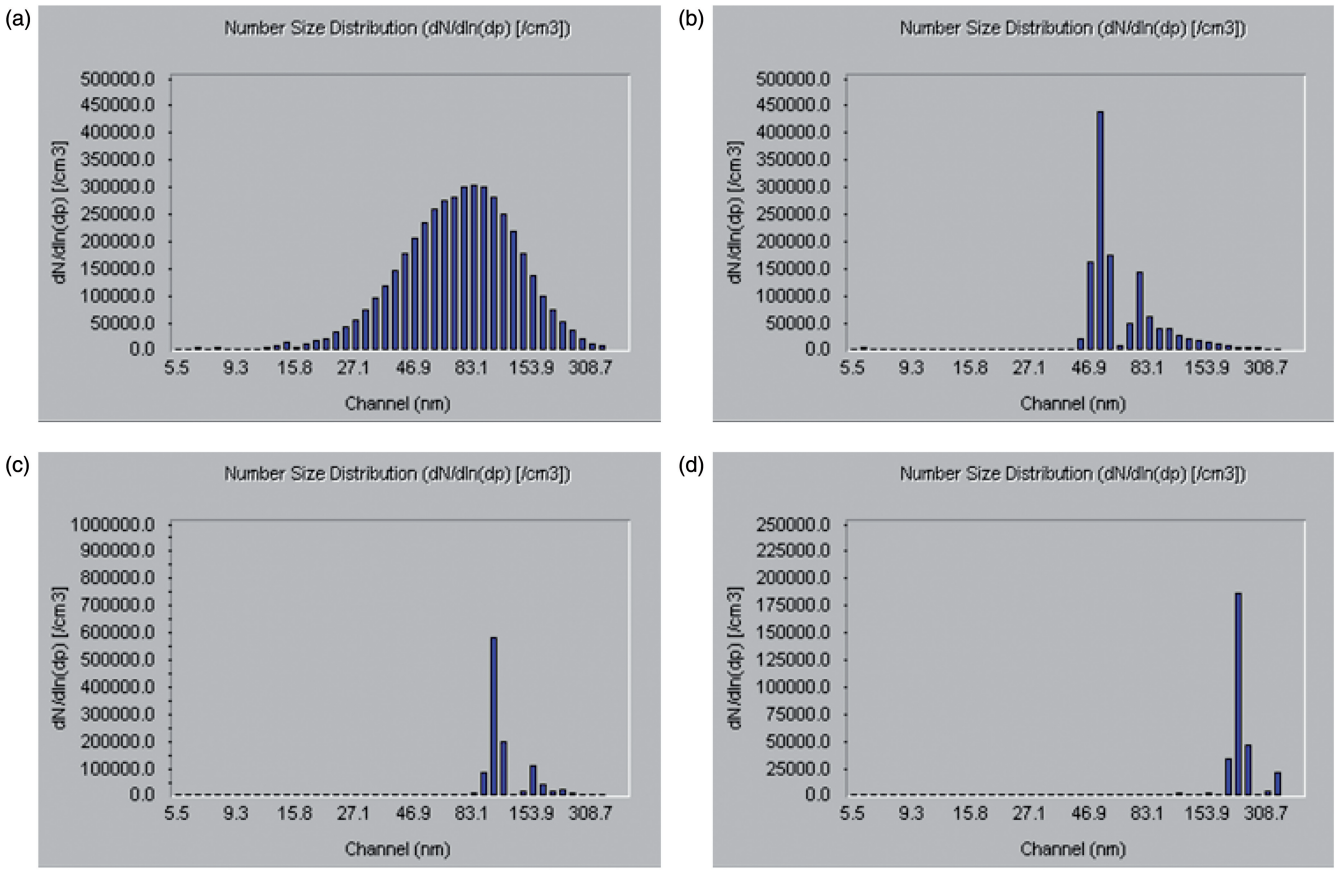

Figure 6. The size distribution of the classified CNTs (a) prior classification, (b) after 51 nm size classification, (c) after 101 nm size classification and (d) after 215 nm size classification.

inspiratory flow rates used in this deposition study. It should be noted that for all the experimental conditions designed in this study that the CNT deposition efficiency in the nasal airway were generally less than 0.1.

Discussion

As shown in Figure 6, the size classified CNTs showed apparent concentration peaks at corresponding channels representing 51, 101 and 215 nm in the SMPS. This result indicates that the CNT aerosols could be successfully size classified by DMA based on their inherent electrical mobility diameter. It is worth noting that although some concentration subpeaks are shown in each classification diameter, the concentrations of these subpeaks were considerably lower in comparison to the main concentration peak. However, questions and issues may still be raised about the forming and effects of these subpeaks on the final result of the deposition study. Based on the principle of the DMA operation (Cheng & Denee, 1981), these subpeaks were formed by doubly or triply charged CNTs with their d_B larger or smaller than the designated classification diameter. These multiply charged CNTs could also be size classified while transiting in the DMA, exiting to the outlet of the DMA, and then being measured by the SMPS. The influence of these multiply charged CNTs on the result of DMA size classification theoretically should be insignificant, since the ratio of the percentage of multiply charged particles to that of singly charged particles is relatively low (Flagan, 2008). Therefore, it ensures that the majority of the classified CNTs coming out of the DMA should have a d_B that is the same as the designated classification diameter. Besides, the experimental method of this deposition study was designed by using only one SMPS channel to track the change of the peak concentration over time. Therefore, focus could be made solely on the designated classification diameter of interest, and those CNTs with d_B away from the designated classification diameter could be omitted automatically; they had a very limit influence on the final deposition data.

As could be noticed from the CNT morphology analysis (Figures 7 and 8), even though CNT aerosols have been size classified, they still could be in a variety of complicated shapes. For SCCNTs (Figure 7), the classified SCCNTs could be a single tube, tangled tube, curved tube, round tube, as well as birdnest-like tubes. In addition, it was found that the physical dimension of the classified SCCNTs were much larger than their designate classification diameter (the reference bar in each CNT subpicture indicates 100 nm). As for the SWCNTs (Figure 8), by contrast, the shape of the classified SWCNTs were relatively more consistent in comparison to the classified SCCNTs. The classified SWCNTs were basically all in circular shapes similar to cotton balls or twisted rubber bands with letter ''O'' or number ''8'' shapes. Similar to the SCCNTs, the physical dimension of the classified SWCNTs were found to be much larger than their designated classification diameter. From this CNT aerosol morphology analysis, it is clearly demonstrated that both SCCNT and SWCNT aerosols are constructed by loose

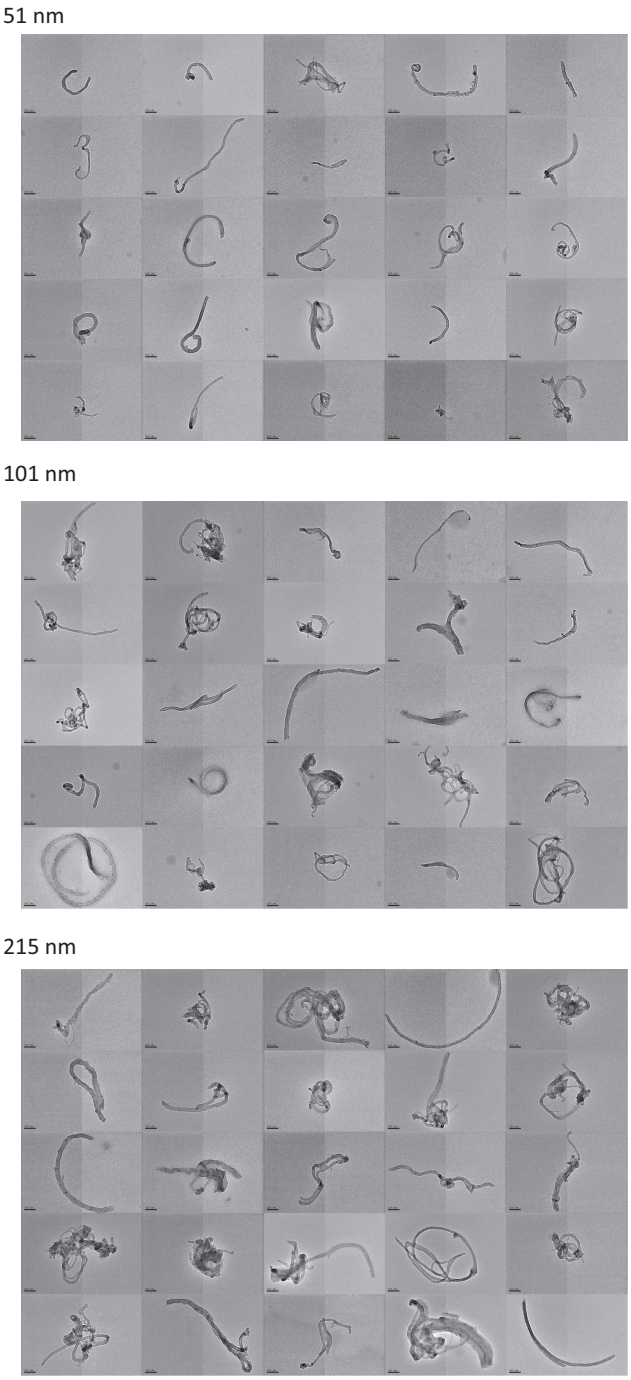

Figure 7. The morphology of the size classified SCCNTs (reference bars in each subpicture represent 100 nm).

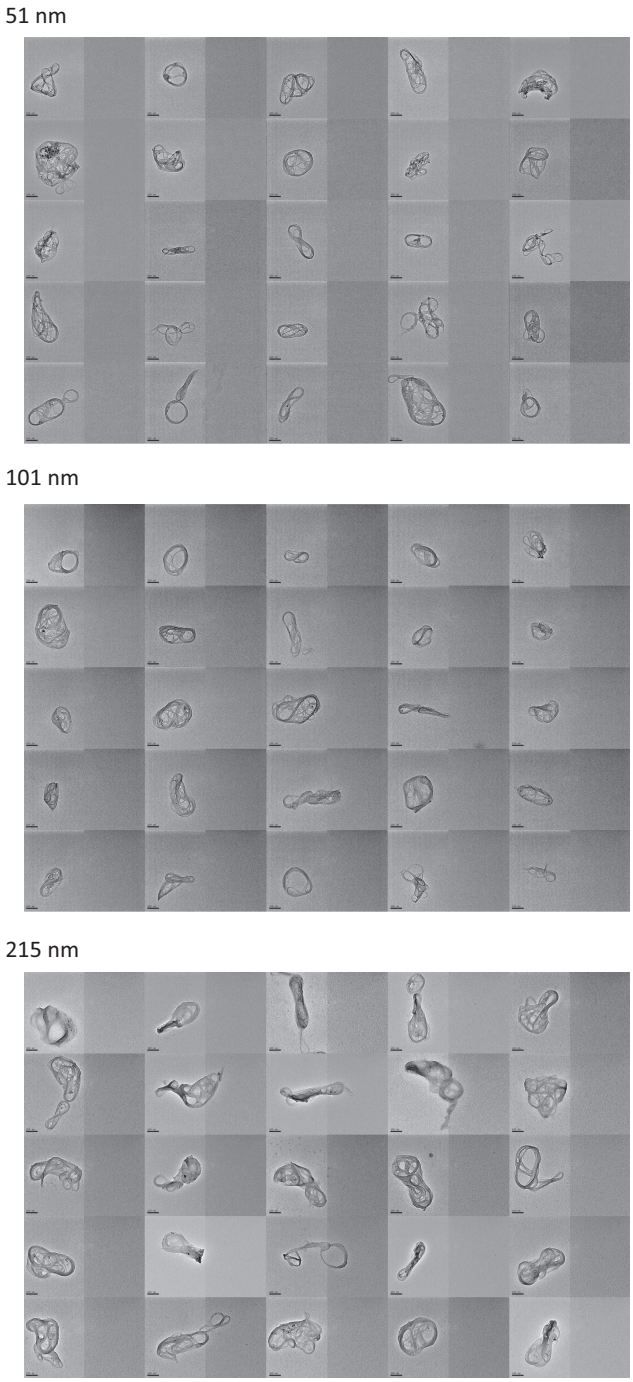

Figure 8. The morphology of the size classified SWCNTs. (reference bars in each subpicture represent 100 nm).

nanotubes with considerable void. Therefore, even though the CNTs dimensions are much larger than the designated classification diameter, their d_B is compromised by their limited mass due to the void in their structure. This statement was also in agreement with what was found in the APM study conducted in this research as shown in the Table 1. As can be seen, given that the density of CNT bulk material is roughly about 2 g/cm^3, the calculated effective density $\rho_{\text{eff CNT}}$ of the size classified CNT aerosols were generally less than 1 g/cm^3. Some published research also found a similar result, which showed a relatively low effective density for CNTs and aggregated nanoparticles (McMurry et al., 2002; Park et al., 2003; Ku et al., 2006; Chen, et al., 2012).

As can be seen in Table 2, the deposition efficiencies of SCCNTs and SWCNTs in the nasal airway expressed no appreciable difference and trend associated with the experimental condition (CNT material, classification diameter and flow rate) used in this deposition study. The nasal deposition efficiencies obtained all ranged around 0–0.1. This result implies that most of the SCCNTs and SWCNTs inhaled into the nasal airway with d_B from 51 to 215 nm will easily pass through the nasal airway and enter the tracheobronchial or even lower airways where possible adverse health effects could be induced. This is not a surprising result because, based on *in vivo* and *in vitro* studies in the literature, aerosols

with diameters within the range of the designated classification diameters used in this study always showed a relatively low deposition efficiency in the nasal airway as compared to some other larger or smaller particles (Cheng et al., 1996; Cheng, 2003). This result might be due to the fact that there is a lack of a strong deposition mechanism for aerosols within this diameter range to deposit in the nasal airway. Figure 10 plots the CNTs deposition efficiency in the human nasal airway as a function of the impaction parameter ($d_{ae}^2 Q$). Also plotted together are deposition data of fiber aerosol and spherical particle previously acquired in our laboratory using the same nasal airway replica (Su et al., 2008). The d_{ae} used for calculating the impaction parameters for size classified CNTs were those listed in Table 1. As can be seen in Figure 10, the continuity of the nasal deposition efficiencies between different experimental data sets was shown fairly well. All the data sets are shown to connect each other smoothly from the large carbon fiber with the length longer than 100 μm to the small CNTs with mobility diameters around 50 nm. Figure 10 also presents no apparent discrepancy between CNT data and the spherical particle data. This result implies that, for the classified CNTs in the size range studied in this research, as long as a CNT has the same d_{ae} as a compact particle (despite the

Table 1. The effective density and aerodynamic diameter of the size classified CNTs.

SCCNT		
Electrical mobility diameter d_B (nm)	Effective density ρ_{eff} (g/cc)	Aerodynamic diameter d_{ae} (nm)
51	0.91 ± 0.01	46.8 ± 0.1
101	0.87 ± 0.01	88.8 ± 0.2
215	0.83 ± 0.02	183.8 ± 1.6
SWCNT		
Electrical mobility diameter d_B (nm)	Effective density ρ_{eff} (g/cc)	Aerodynamic diameter d_{ae} (nm)
51	0.92 ± 0.02	47.2 ± 0.2
101	0.93 ± 0.01	94.0 ± 0.3
215	0.90 ± 0.01	194.4 ± 0.9

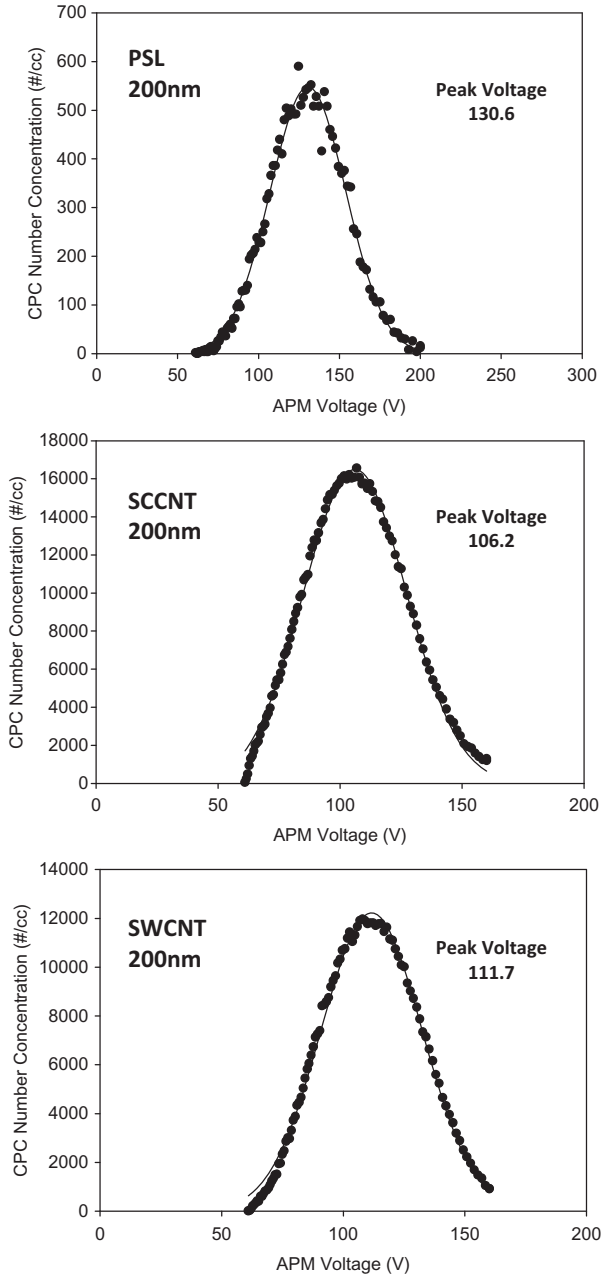

Figure 9. Examples of the results from DMA–APM study.

Table 2. The deposition efficiency of SCCNT and SWCNT in the human nasal airway.

SCCNT			
Flow rate Q L/min)	Electrical mobility diameter (nm)		
	51	101	215
15	0.07 ± 0.08 (1.12)	0.03 ± 0.04 (1.06)	0.06 ± 0.04 (1.00)
30	0.04 ± 0.13 (1.13)	0.01 ± 0.03 (1.07)	0.04 ± 0.02 (1.00)
43.5	0.05 ± 0.11 (1.10)	0.03 ± 0.03 (1.01)	0.07 ± 0.02 (1.00)
SWCNT			
Flow rate Q (L/min)	Electrical mobility diameter (nm)		
	51	101	215
15	0.03 ± 0.08 (1.13)	0.06 ± 0.05 (1.05)	0.03 ± 0.05 (1.05)
30	0.03 ± 0.02 (1.16)	0.01 ± 0.05 (1.06)	0.05 ± 0.04 (1.00)
43.5	0.04 ± 0.04 (1.11)	0.05 ± 0.03 (1.02)	0.03 ± 0.02 (1.00)

The numbers in brackets are the particle delivery efficiency correction factors acquired.

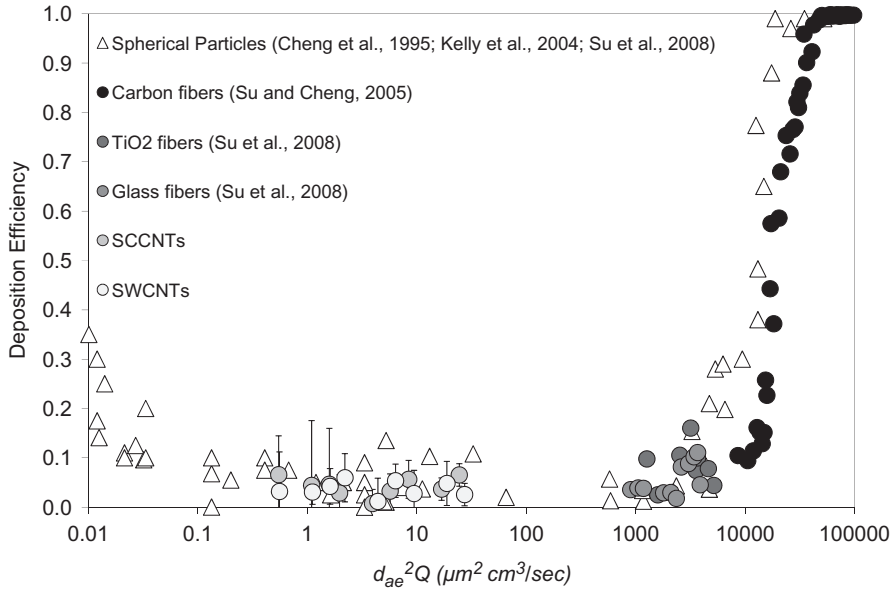

Figure 10. The deposition efficiency of CNTs in the human nasal airway as a function of impaction parameter.

fact that their morphologies are complicated and their physical dimensions are much larger than their designated classification diameter), the CNT will behave similarly to the compact particle, which will result in a comparable deposition efficiency in the human nasal airway.

Conclusion

In this study, two types of CNT materials (SCCNTs and SWCNTs) were aerosolized, size classified, characterized and then used for conducting nasal airway deposition study. The experimental result obtained showed that CNT aerosols can be ideally size classified by designated classification diameter using a DMA. The size classified CNTs generally presented a complicated shape morphology, low effective density and slightly smaller aerodynamic diameter than the relevant electrical mobility diameter. The nasal deposition data acquired in this study showed that the deposition efficiency of CNTs in the nasal airway were all below 0.1, which implies that most of the CNTs inhaled could easily penetrate through the nasal airway and further transit down to the lower airways. The experimental scheme employed in this deposition study can be a useful experimental approach to apply on other human airway deposition studies using different airway sections with additional types of CNT or nanoparticle materials.

Acknowledgements

The authors are grateful to Eileen Kuempel and Pramod Kulkarni at NIOSH for developing the concept of this research project; Bean Chen and Bahman Asgharian for useful discussion on the deposition data; and Bon-Ki Ku with special thanks for helping with conducting the APM study.

Declaration of interest

This project was sponsored by NIOSH contract 254-2010-M-36304, 214-2012-M-52048 and research grant R01OH010062.

References

Chen BT, Schwegler-Berry D, McKinney W, et al. (2012). Multi-walled carbon nanotubes: sampling criteria and aerosol characterization. Inhal Toxicol 24:798–820.

Cheng KH, Cheng YS, Yeh HC, Swift DL. (1995). Deposition of ultrafine aerosols in the head airways during natural breathing and during simulated breath holding using replicate human upper airway casts. Aerosol Sci Technol 23:465–74.

Cheng YS, Denee PB. (1981). Physical properties of electrical mobility classified aerosols. J Colloid Interf Sci 80:284–93.

Cheng YS, Yeh HC, Guilmette RA, et al. (1996). Nasal deposition of ultrafine particles in human volunteers and its relationship to airway geometry. Aerosol Sci Technol 25:274–91.

Cheng YS, Holmes TD, Gao J, et al. (2001). Characterization of nasal spray pumps and deposition pattern in a replica of human nasal airway. J Aerosol Med 14:267–80.

Cheng YS. (2003). Aerosol deposition in the extrathoracic region. Aerosol Sci Technol 37:659–71.

Dahm MM, Evans DE, Schubauer-Berigan MK, et al. (2012). Occupational exposure assessment in carbon nanotube and nanofiber primary and secondary manufacturers. Ann Occup Hyg 56:542–56.

De Volder MFL, Tawfick SH, Baughman RH, Hart AJ. (2013). Carbon nanotubes: present and future commercial applications. Science 339: 535–9.

Donaldson K, Aitken R, Tran L, et al. (2006). Carbon nanotubes: a review of their properities in relation to pulmonary toxicology and workplace safety. Toxicol Sci 92:5–22.

Endo M, Strano MS, Ajayan PM. (2008). Potential applications of carbon nanotubes. CNT 111:13–61.

Flagan RC. (2008). Differential mobility analysis of aerosol: a tutorial. KONA Powder Part J 26:254–68.

Kelly JT, Asphgrian B, Kimbell JS, Wong BA. (2004). Particle deposition in human nasal airway replicas manufactured by different methods. Part II: ultrafine particles. Aerosol Sci Technol 38:1072–9.

Ku BK, Emery MS, Maynard AD, et al. (2006). In situ structure characterization of airbone carbon nanofibers by a tandem mobility-mass analysis. Nanotechnology 16:3613–21.

McMurrry PH, Wang X, Park K, Ehara K. (2002). The relationship between mass and mobility for atmospheric particles: a new technique for measuring particle density. Aerosol Sci Technol 36:227–38.

Mercer RR, Hubbs AF, Scabilloni JF, et al. (2010). Distribution and persistence of pleural penetrations by multi-walled carbon nanotubes. Part Fibre Toxicol 7:1–11.

Mitchell LA, Gao J, Wal RV, et al. (2007). Pulmonary and systemic immune response to inhaled multiwalled carbon nanotubes. Toxicol Sci 100:203–14.

Muller J, Huaux F, Moreau N, et al. (2005). Respiratory toxicity of multi-wall carbon nanotubes. Toxicol Appl Pharmacol 207:221–31.

National Institute for Occupational Safety and Health (NIOSH). (2013) Current intelligence bulletin: occupational exposure to carbon nanotubes and nanofibers. DHHS (NIOSH) Publication No.2013-145.

NCRP. (1997). National council on radiation protection and measurements: deposition, retention and dosimetry of inhaled radioactive substances, NCRP Report No. 125, National council on radiation protection and measurements, Bethesda, MD.

Parish A. (2011). Production and applications of carbon nanotubes, carbon nanofibers, fullerenes, graphene and nanodiamonds: a global technology survey and market analysis. Innovative Research and Products, Inc Report.

Park K, Cao F, Kittelson DB, McMurrry PH. (2002). Relationship between particle mass and mobility for diesel exhaust particles. Environ Sci Technol 37:577–83.

Pauluhn J. (2010). Subchronic 13-week inhalation exposure of rats to multiwalled carbon nanotubes: toxic effects are determined by density of agglomerate structures, not fibrillar structures. Toxicol Sci 113: 226–42.

Peto J, Doll R, Howard SV, et al. (1977). A mortality study among workers in an English asbestos factory. Br J Ind Med 34:169–73.

Porter DW, Hubbs AF, Mercer RR, et al. (2010). Mouse pulmonary dose- and time course-responses induced by exposure to multi-walled carbon nanotubes. Toxicology 269:136–47.

Su WC, Cheng YS. (2005). Deposition of fiber in the human nasal airway. Aerosol Sci Technol 39:888–901.

Su WC, Wu J, Cheng YS. (2008). Deposition of man-made fiber in a human nasal airway. Aerosol Sci Technol 42:173–81.

Subramaniam RP, Richardson RB, Morgan KT, et al. (1998). Computational fluid dynamics simulations of inspiratory airflow in the human nose and nasopharynx. Inhal Toxicol 10:91–120.

Wang X, Li Q, Xie J, et al. (2009). Fabrication of ultralong and electrically uniform single-walled carbon nanotubes on clean substrates. Nano Lett 9:3137–41.

Zwartz GJ, Guilmette RA. (2001). Effect of flow rate on particle deposition in a replica of a human nasal airway. Inhal Toxicol 13: 109–27.